

Local relaxations and electric-field gradient at the Cd site in heavily doped Si:Cd

R. A. Casali and M. A. Caravaca

Departamento de Fisica, Facultad de Ciencias Exactas, Universidad Nacional del Nordeste, 9 de Julio 1449, (3400) Corrientes, Argentina

C. O. Rodriguez

Instituto de Liquidos y Sistemas Biologicos (IFLYSIB), Grupo Fisica del Solido, Casilla de Correo 565, La Plata (1900), Argentina
(Received 6 June 1996)

The full-potential linear muffin-tin orbitals method, within the local density approximation to density functional theory has been employed to study the relaxations, anharmonicities of local modes, and the possible appearance of an electric-field gradient (EFG) at substitutional Cd in silicon. Using the supercell approach, the total energy variations associated to the T_d , D_{2d} , and C_{2v} local modes, which involve silicon nearest neighbors (NN) to the Cd impurity were calculated theoretically, once the system achieved its relaxed energy minimum at a 4% volume dilation. An outward breathing relaxation of 0.12 Å (NN) and 0.05 Å (next-nearest neighbor) Si atoms around Cd was found to be the minimum energy (4% volume dilation and the T_d distortion), although the D_{2d} mode showed a possible (but very small) further relaxation of 0.003 Å, similar to what has been found in the silicon neutral vacancy. At this energy minimum a C_{2v} sliding mode distortion of Cd was then investigated. This mode showed a strong anharmonicity with a double-well structure and an associated electric-field gradient. On the basis of the agreement between our calculated EFG and the values measured with time-differential perturbed-angular-correlation techniques together with the experimentally observed temperature dependence, we propose that of the models suggested in the literature, a dynamic Jahn-Teller mechanism could describe the appearance of the EFG. [S0163-1829(96)07047-6]

I. INTRODUCTION

Time-differential perturbed-angular-correlation (TDPAC) experiments¹⁻³ have given information on the behavior of Cd impurities implanted on Si. The main results of TDPAC experiments for Si:Cd are as follows: (a) At low temperature there is a sizable electric-field gradient (EFG) at the Cd site. (b) At high temperature TDPAC gives evidence of a vanishing EFG consistent with the cubic symmetry of the Si host lattice.¹ Furthermore, Hall experiments provide evidence about the presence of at least two deep levels in the Si gap associated with Cd impurity.⁴ Many mechanisms have been proposed to explain the observed value of the EFG at low temperatures: (a) The presence of electronic holes, more or less bound to the radioactive acceptor ion,¹ (b) surface charge effects,² (c) Cd-charged states associated to possible Jahn-Teller distortions,⁵ and (d) "after effects" on the electron-capture decay of ¹¹¹In to ¹¹¹Cd.⁶

At present the simple Si:Cd system is not completely characterized experimentally and very poorly characterized theoretically. It is the aim of this work to give an alternative framework for results previously found in silicon clusters obtained by using the extended Hückel theory⁷ and try to give insight into the microscopic mechanisms involved.

We have used the first-principles full-potential linear muffin-tin orbital (FP-LMTO) method within the local density approximation (LDA) to density functional (DF) theory. A supercell geometry approach that has proven (using diverse first principles approaches) successful for the study of the electronic structure, relaxations, vibrational properties, and path of migrations of defects⁸⁻¹² was used to model our system.

Other schemes have been used to evaluate lattice dynamical properties in the context of defects in semiconductors (i.e., *ab initio* molecular dynamics^{13,14} and *ab initio* in conjunction with Keating model or valence force field^{8,15,16}).

In this paper, the electronic structure, bonding properties, relaxations, and frequencies of vibrations of the host T_d , D_{2d} , and C_{2v} local modes associated to the nearest neighbor (NN) to the Cd defect in Si, as well as the C_{2v} sliding mode of Cd are presented. The latter is labeled as Cd C_{2v} and corresponds to a displacement of the Cd atom along any of the equivalent directions to (100). Because it has been well characterized and due to its close relation to the Si:Cd problem, the substitutional neutral vacancy in silicon (Si: V^0) was also analyzed and used as a reference. In Sec. II a short description of the calculational procedure is described. In Secs. III and IV the results obtained for the unrelaxed, relaxed, and relaxed-distorted situations are analyzed, including the possible appearance of an EFG on a Cd C_{2v} distortion. In Sec. V we consider results for the frequencies and the force constants associated with the breathing T_d , D_{2d} , and C_{2v} local mode distortions studied.

II. METHOD OF CALCULATION

For the calculations presented here we used a fast and precise FP-LMTO code by Methfessel¹⁷ within the LDA and the Hedin-Lundqvist exchange-correlation potential. In the FP-LMTO, no shape approximations are made for either the charge density or the potential. As is customary for a LMTO approach, the basis for the wave functions consists of atom-centered Hankel functions that are augmented by numerical solutions of the radial one-electron equation within the non-

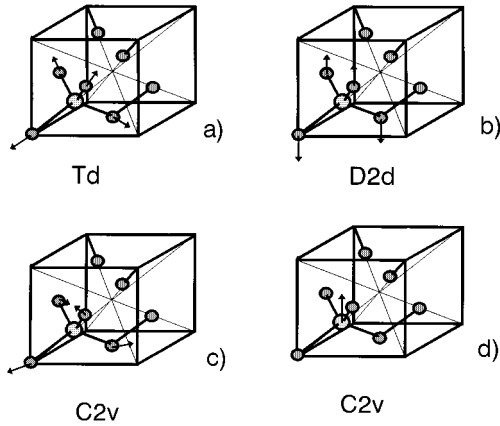


FIG. 1. Local mode distortion pattern for host atoms: (a) breathing relaxation, (b),(c) low symmetry distortions, and (d) sliding mode for the substitutional defect.

overlapping atomic spheres. The charge density is represented in the interstitial region by fitting a linear combination of Hankel functions to the values and slopes on the sphere boundaries. To provide sufficient variational freedom, it is essential in the method to extend the basis using LMTO's with various localizations. The envelope function decays as $e^{-\kappa r}$, where $-\kappa^2$ is the kinetic energy of the Hankel function envelope.

The calculations are accomplished with supercells containing 16 atoms (Si_{15}Cd). A 32-atom supercell was used for tests of convergence. In the first case, the primitive cell corresponds to a fcc lattice with $a = 10.86 \text{ \AA}$.

The calculations were carried out in one panel. The following orbitals were taken as valence electrons: Si $3s$ and $3p$, and Cd $5s$ and $4d$. Tests were made to check the possible need of inclusion of semicore states with the use of a second panel. We have used $-\kappa^2 = -0.01, -1.0, \text{ and } -2.3$. The basis set included 208 and 416 LMTO's for the 16- and 32-atom supercell, respectively. The muffin-tin (MT) radii were 2.52, 1.92, and 2.13 a.u. for Cd, Si (NN), and Si [next-nearest neighbors (NNN)], respectively, for the atmospheric pressure filling. Empty spheres were added in order to achieve better space filling. The resulting sphere packing ratio ($V_{\text{MT}} / V_{\text{total}}$) was $\approx 55\%$. The muffin-tin sphere radii were scaled to preserve this packing ratio in all cases where volume was varied.

The local mode distortion pattern studied is depicted in Fig. 1. These were proposed first by Watkins¹⁸ for the vacancy in silicon. We have estimated the mean square displacements of the local modes using Debye theory of harmonic oscillators¹⁹ to be $\langle u_{\text{Si}} \rangle = 0.04$ and 0.07 \AA for $T = 0$ and 293 K, respectively. We used distortions in the range of 0.07 \AA for the NN of Cd. The MT radii were chosen so as to avoid any kind of superposition between atoms and empty spheres at the range of estimated atomic displacements for all local modes considered. In the case of the Cd C_{2v} mode, because of the strong anharmonicity observed, we selected the range of displacements $\langle u_{\text{Cd}} \rangle = 0.15 \text{ \AA}$. For the local distortion calculations presented here, the total energies were calculated for a sufficient number of displacements and a least-squares fit was applied, from which anharmonicities and the vibrational frequencies were derived. Expansions

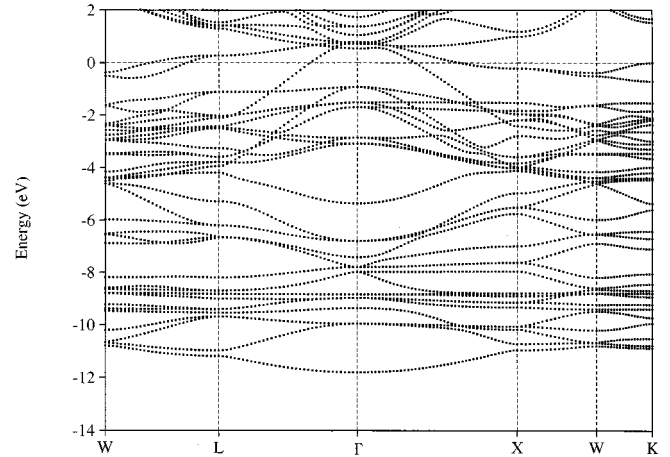


FIG. 2. Supercell band structure of Si_{15}Cd , plotted along representative high-symmetry directions.

containing up to the cubic term were necessary for the fitting of all modes, except in the special case of the strong anharmonic Cd C_{2v} , where eight terms were used.

The symmetry corresponding to the less symmetric mode, C_{2v} , was used for all calculations, in order to preserve reciprocal space sampling precision. The points in the Brillouin zone were chosen according to the special points scheme. Twenty special points for the 16-atom supercell were used in the irreducible wedge of the Brillouin zone. Due to the intrinsic dispersion of defect states introduced in the band structure with the supercell technique, and since these levels are partially filled, our system was treated as metallic. The sampling points used are considered sufficient and were selected after studies of total energy convergence tests were carried out with denser samplings.

The electric field gradient was calculated²⁰ using the non-spherical part ($l=2$) of the crystalline Hartree potential, from which the second derivative tensor $V_{i,j} = \partial^2 V_{H,l=2} / \partial x_i \partial x_j$ was obtained. The corresponding eigenvalues of $V_{i,j}$ are denoted by V_{xx}, V_{yy}, V_{zz} with $|V_{xx}| \leq |V_{yy}| \leq |V_{zz}|$. The EFG by definition is V_{zz} , while an asymmetry parameter is defined as $\eta = (V_{xx} - V_{yy}) / V_{zz}$ and lies in the range $[0,1]$ (the tensor is defined as traceless). The quadrupolar frequency ν_Q was calculated as $\nu_Q = e Q_{\text{Cd}} V_{zz} / h$, where Q_{Cd} is the experimental quadrupolar moment²¹ of the Cd nuclei in the intermediate state $I = \frac{5}{2}$, e the electron charge, and h is Planck's constant.

III. UNRELAXED Si:CD LATTICE: ELECTRONIC STRUCTURE AND BONDING PROPERTIES

In this section we will analyze results for the unrelaxed Si:Cd (i.e., a Cd impurity is introduced at a substitutional Si host site (Si_{15}Cd)). Figure 2 shows the band structure plotted along symmetry directions of the Si fcc. It corresponds to a slightly distorted folded-in band structure of Si, with the introduction of defect states in the Si band gap. These states have dispersion due to our limited supercell and had to be treated as metallic, as already mentioned.

Figures 3(a) and 3(b) show our total and partial density of states (DOS and DOSP) for Si:Cd. Results for DOS (inset)

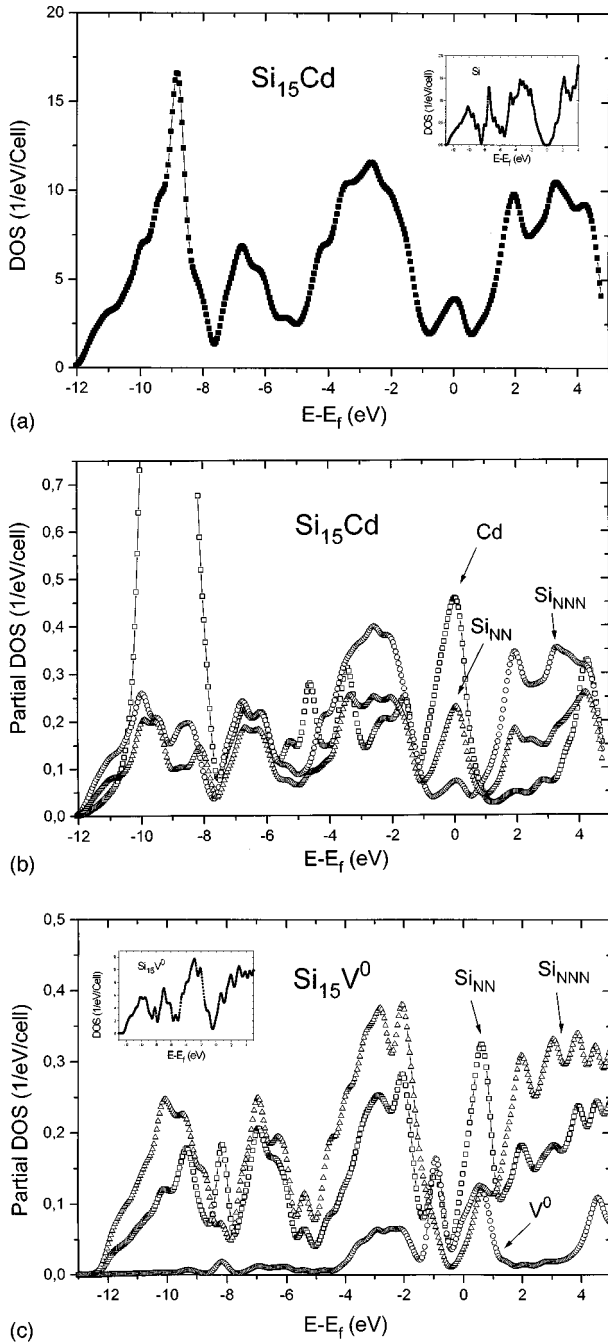


FIG. 3. (a) Total density of states (DOS) of Si_{15}Cd . The inset corresponds to pure Si. (b) Partial density of states (PDOS) of Si_{15}Cd . (c) Partial DOS of Si_{15}V^0 (the inset shows total DOS for the same system).

and DOSP for $\text{Si}:\text{V}^0$ are shown in Fig. 3(c). E_f indicates our determined Fermi energy.

Two extra peaks can be individualized in the total DOS curve of Si_{15}Cd in Fig. 3(a), which are not in the host-Si DOS [compare with the inset of Fig. 3(a)]: a narrow and high valued one, located at -8.8 eV from E_f , and another that falls within the energy gap of the undoped host. Figure 3(b) serves to analyze the character of these peaks. The first one has contributions that come mainly from the Cd $4d$ orbitals and because of the relatively small dispersion of the corresponding band reflects a small bonding of the impurity with

the surrounding atoms. The second peak that falls inside the host-Si energy gap has contributions that are mainly derived from the Cd atom and to a smaller degree from the surrounding four Si NN. The contributions to this peak from Si NNN appear unimportant. This gives an idea of the degree of localization of the defect states. In Fig. 3(c), which serves for comparison the DOSP for the $\text{Si}:\text{V}^0$ case shows a different pattern since the main contribution to the defect states in the gap comes mainly from Si NN surrounding the vacancy.

IV. RELAXATIONS, LOCAL DISTORTIONS, AND C_{2v} SLIDING MODE IN $\text{Si}:\text{Cd}$

The introduction of the defect in the lattice induces a strain field that extends throughout the crystal. The relaxation of surrounding atoms lowers the lattice energy. This effect was simulated in our supercell calculation by isotropic lattice relaxation, searching the $E_{\text{tot}}(V_{\text{supercell}})$ minima. We found a 4% volume dilation. This implies that NNN move outward 0.05 Å from Cd. As a comparison, we applied the law of relaxations that for the different shells of atoms surrounding the As substitutional impurity in Si was proposed by Scheffler and Dabrowski⁸ using the Keating approach. We obtain a radial relaxation of the same order, 0.035 Å. The quantitative difference could be due to processes that are not taken into account in the Keating model.

But, the most important strain suffered by the lattice after the introduction of the defect is localized in the NN host atoms. We have then, first, distorted the lattice around the Cd center following a T_d symmetry, Fig. 1(a). After the minima of $E_{\text{tot}}(u = u_{T_d})$ is found, we have allowed for two other different distortions ($u = u_{T_d,0} + u_i$) of NN silicons ($i = D_{2d}$ and C_{2v}) as shown in Figs. 1(b) and 1(c). From the fitted curve of $E_{\text{tot}}(u)$ to a polynomial, force constants, distances of equilibrium and the vibrational frequencies can be calculated for each studied mode.

A charge density contour plot of the $\text{Si}:\text{Cd}$ system with Cd at the substitutional, after the T_d relaxation, is shown in Fig. 4. The charge redistributes shifting to bonds between NN and NNN host shells.

A T_d outward relaxation of 0.12 Å (5% of NN distance) is predicted. We have found that this relaxation does not depend on the cell size when comparing a small 8-atom supercell to the 16-atom one. This coincides with the behavior observed in extended x-ray-absorption fine-structure measurements (EXAFS) for As implanted on silicon²² with three very different concentrations: 0.1%, 0.7%, and 7%. In particular, the last impurity concentration is analogous to the 16-atom supercell studied here. However, in that case the predicted NNN radial relaxations were in the range of 0.005 – 0.01 Å (an order of magnitude smaller than our prediction for Cd). On the other hand, parameter-free self-consistent Green's-function calculations by Scheffler⁸ for that case predicted an expansion of 0.03 ± 0.01 Å. Table I resumes our results for the different relaxations here considered. Similar, outward relaxations were also found by Scheffler and Dabrowski in other doped systems: $\text{Si}:\text{S}^0$ (1.2%) (Ref. 23) and $\text{Si}:\text{As}^+$ (1.7%).²³

The D_{2d} mode is slightly anharmonic and shows a small relaxation, $u_0 = -0.003$ Å. The C_{2v} host mode, Fig. 1(c), is symmetric and harmonic. This is a natural consequence of

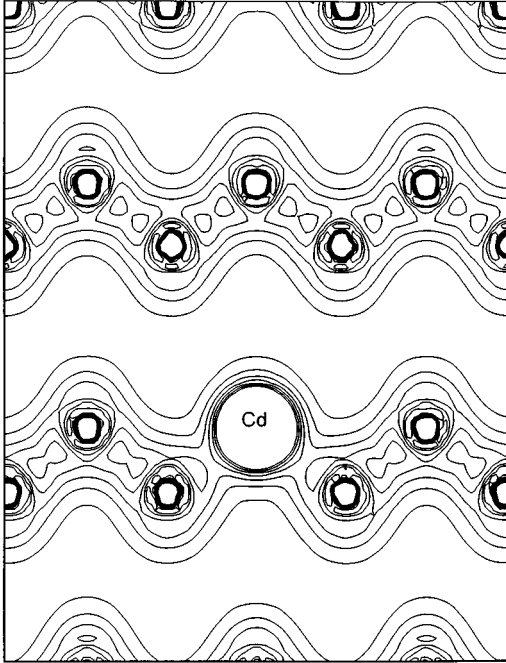


FIG. 4. Contour map of valence charge density of Si_{15}Cd in the plane $[110]$, after T_d relaxation, with contour steps of $0.015 e/\text{a.u.}^3$.

the way the bonds between Si NN and NNN are distorted. This mode is the most dependent with the cell size.

The most interesting structural reconstruction found in this study is the strong anharmonicity of the potential energy felt by the Cd atom when it is displaced in the equivalent directions (100). The structure becomes unstable. A double well is predicted in each direction (a total of three exist) with a barrier on the order of a few meV as shown in Fig. 5. The minimum energy is at $u(C_{2v})=0.017 \text{ \AA}$ (see Table I). The height of this barrier will have a crucial incidence in the dynamics and the Jahn-Teller restructuring of the Cd atom. Because of its mass, the Cd atom will possess a low kinetic energy. This will be of the order of 1.5 meV if estimated considering the Cd atom in a quadratic potential with $k_b=1 \text{ eV/\AA}^2$ (extracted from an eight-term polynomial fit to the double-well potential). It is then expected to be localized at one minima of the energy potential curve. Since charged surface states could exert an external electric field over the probe, and localize it on one side of the double-well curve, the appearance of a sizable EFG could be explained in this manner. But, the low barrier height inhibits the process of localization: there exists a possibility of hopping between the wells, a process favored by temperature. Also, at high tem-

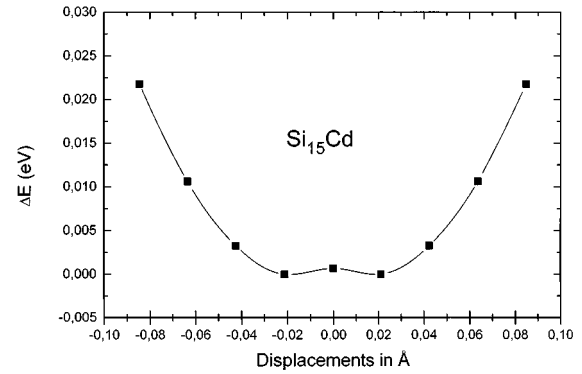


FIG. 5. Double-well potential felt by the Cd probe when it is displaced along each equivalent direction (100).

perature the anharmonicity of the Si NN D_{2d} mode could tend to suppress the double well. In this way one can explain the results for the strong dependence of the EFG with temperature observed experimentally.¹⁻³

We have calculated the EFG at the Cd site and the corresponding ν_Q using the nuclear quadrupolar moment $Q=0.83 \text{ b.}^{21}$ A quadrupolar frequency of $\nu_Q=22 \text{ MHz}$ was obtained for a displacement of the Cd atom $u(\text{Cd}-C_{2v})=0.017 \text{ \AA}$, a value that is extremely sensitive to the size of the displacement. Our predicted EFG is close to the $T=24 \text{ K}$ experimental value of 20 MHz obtained in intrinsic silicon samples.¹

V. FREQUENCY AND INTERATOMIC FORCE CONSTANTS

The changes in total energy for the relaxations around the defect already described determinate the magnitude of force constants and consequently, vibrational frequencies. These are shown in Table I.

For the T_d case the calculated force constant and frequency for the Si_7Cd supercell (which represents a 12.5% dilution of the impurity) are $k_b=50.6 \text{ eV/\AA}^2$, $\nu[T_d]=10.49 \text{ THz}$. If we take the Si_{15}Cd supercell we reduce to 6.25 the percentage of Cd, and obtain $k_b=48 \text{ eV/\AA}^2$ and $\nu[T_d]=10.2 \text{ THz}$. These values are close to those found in the literature, $k_b=47 \text{ eV/\AA}^2$ for Si:As^+ and $k_b=53 \text{ eV/\AA}^2$ Si:P^+ .²³ On the other hand pure silicon has a higher value of $k_b=63.4 \text{ eV/\AA}^2$.

For the D_{2d} distortion the calculated force constants are $k_b=41 \text{ eV/\AA}^2$ for Si_7Cd , which increases to 44 eV/\AA^2 for Si_{15}Cd . These values are lower than those of the T_d breathing mode. The k_b for the C_{2v} distortion of the Si host is the most sensible to supercell size, changing from 36 (Si_7Cd) to

TABLE I. Calculated relaxations, force constants, and vibrational frequencies corresponding to host modes; relaxations and quadrupolar frequency in the Cd site correspond to the defect after Jahn-Teller distortion. The units are in \AA , eV/\AA^2 , and THz; quadrupolar frequency is expressed in MHz.

	T_d			D_{2d}			C_{2v}			Cd- C_{2v}	
	u	k_b	ν (THz)	u	k_{bd}	ν (THz)	u	k_b	ν (THz)	u	ν_Q (MHz)
Si_{15}Cd	+0.12	48	10.2	-0.003	44	9.8	0.0	42	9.6	+0.017	21
Si_7V^0	-0.005	23	7.1	-0.004	41	9.4	0.0	33	8.5		

44 eV/Å² (Si₁₅Cd). It is interesting to note that for the T_d distortion of the neutral vacancy we obtain $k_b=22.4$ eV/Å² [experimental estimations give 20.4 and 27.2 eV/Å² (Ref. 24)], which is half the value for Si:Cd, while for the D_{2d} and C_{2v} cases the values for Si:Cd and Si:V⁰ are of the same order.

VI. CONCLUSIONS

Several models have been proposed in the literature to interpret the temperature dependence of the EFG, which is observed in TDPAC experiments for the Cd impurity implanted in Si.

Through the evaluation of the variations of the total energy we have studied possible local mode distortions of NN silicon atoms. The minimum energy of the system includes an outward breathing relaxation of 0.12 Å (and 0.05 Å) for the NN and NNN silicon atoms, respectively, with a further (very small) D_{2d} mode relaxation of 0.003 Å. The magnitude of the force constants are found for each of the studied local modes. We have found that a further C_{2v} sliding mode distortion of Cd showed a strong anharmonicity with a double-

well structure that gave rise to the appearance of an EFG. The EFG was found to be very sensitive to the magnitude of the displacement of Cd atom with a value close to the $T=24$ K experimental prediction for $u=0.017$ Å.

On the basis of these findings, we speculate that at very low temperatures, due to its heavy mass, the Cd atom could be localized at one minima with an associated sizable EFG. This process could be enhanced by charge surface states that could exert an electric field over the probe and localize it on one side of the double well. The small barrier height of the double well could allow a hopping of the Cd with temperature that could make the EFG disappear as temperature increases. In this way we identify the dynamic Jahn Teller effect from all models proposed as an explanation for the TDPAC experimental findings.

ACKNOWLEDGMENTS

The authors are grateful to Dr. S. Sferco and Dr. M.C. Passeggi for valuable and stimulating discussions. This work was partially supported by Secretaria de Ciencia y Tecnica of the Universidad Nacional del Nordeste, Project No. 42-01-3.

-
- ¹A. Pasquevich and R. Vianden, Phys. Rev. B **35**, 1560 (1987).
²D. Forkel, F. Mayer, W. Witthun H. Wolf, M. Deicher, and M. Uhrmacher, Hyperfine Interact. **35**, 715 (1987).
³G.J. Kemerink, F. Pleiter, and M. Mohsen, Hyperfine Interact. **35**, 707 (1987).
⁴S. S. Dyunaidov, N.A. Urmanov, and M.V. Gafurova, Phys. Status Solidi A **66**, K79 (1981), and references therein.
⁵H. Wolf, S. Deubler, D. Forkel, F. Meyer, M. Uhrmacher, and W. Witthuhn, Mater. Sci. Forum **38-41**, 463 (1989).
⁶M. Deicher, G. Grüber, E. Recknagel, Th. Wichert, and D. Forkel, Nucl. Instrum. Methods B **13**, 499 (1986).
⁷M. C. Passeggi, J. S. Sferco and M. A. Caravaca, *Proceeding of the 5th Brazilian School on Semiconductor Physics, San Pablo, Brazil, 1991*, edited by J. R. Leite, A. Fazzio, and A.S. Chaves (World Scientific, Singapore, 1991), pp. 530–534.
⁸M. Scheffler and J. Dabrowski, Philos. Mag. A **58**, 107 (1988).
⁹U. Scherz and M. Scheffler, *Semiconductors and Semimetals* (Academic, New York, 1993), Vol. 38, p. 1.
¹⁰C. G. Van de Walle, P. J. Denteneer, Y. Bar-Yam, and S. Pantelides, Phys. Rev. B **39**, 10 791 (1989); C. G. Van de Walle, in *Semiconductors and Semimetals* (Academic, New York, 1991), Vol. 34, p. 585.
¹¹Y. Bar-Yam and J. D. Joannopoulos, Phys. Rev. Lett. **52**, 1129 (1984).
¹²S. Froyen and A. Zunger, Phys. Rev. B **34**, 7451 (1986).
¹³R. Car and M. Parrinello, Phys. Rev. Lett. **55**, 2471 (1985).
¹⁴P. E. Blochl, C. G. Van de Walle, and S. T. Pantelides, Phys. Rev. Lett. **64**, 1401 (1990).
¹⁵P. N. Keating, Phys. Rev. **145**, 637 (1966).
¹⁶R. M. Martin, Phys. Rev. B **1**, 4005 (1970).
¹⁷M. Methfessel, Phys. Rev. B **38**, 1537 (1988); M. Methfessel, C.O. Rodriguez, and O.K. Andersen, *ibid.* **40**, 2009 (1989).
¹⁸G. D. Watkins, *Lattice Defects in Semiconductors 1974*, IOP Conf. Proc. No. 23 (Institute of Physics, London, 1975), p. 1.
¹⁹K. Kunc and R. M. Martin, in *Ab-initio Calculation of Phonon Spectra*, edited by J. T. Devreese, V. E. Van Doren, and P. E. Van Camp (Plenum Press, New York, 1983), pp. 65–99.
²⁰N.E. Christensen, A. Svane, M. Fanciulli, G. Weyer, M. Methfessel, and C.O. Rodriguez, Bull. Am. Phys. Soc. **41**, 788 (1996).
²¹P. Herzog *et al.*, Z. Phys. A **294**, 13 (1980).
²²A. Erbil, W. Weber, G.S. Cargill III, and R.F. Boehme, Phys. Rev. B **34**, 1392 (1986).
²³M. Scheffler, Physica B **146**, 176 (1987).
²⁴G. G. De Leo, W. B. Fowler, and G. D. Watkins, Phys. Rev. B **29**, 3193 (1984); M. Scheffler, J. P. Vigneron, and G. B. Bachelet, *ibid.* **31**, 6541 (1985).